PHYSICAL REVIEW D **92,** 075014 (2015)

Electroweak baryogenesis in the framework of the effective field theory

Fa Peng Huang[1] and Chong Sheng Li[1,2,*]

[1]*School of Physics and State Key Laboratory of Nuclear Physics and Technology, Peking University, Beijing 100871, China*

[2]*Center for High Energy Physics, Peking University, Beijing 100871, China*

(Received 3 August 2015; published 13 October 2015)

We study the electroweak baryogenesis in the framework of the effective field theory. Our study shows that by introducing a light singlet scalar particle and a dimension-5 operator, it can provide the strong first order phase transition and the source of the *CP*-violation during the phase transition, and then produce abundant particle phenomenology at zero temperature. We also show the constraints on the new physics scale from the observed baryon-to-photon ratio, the low-energy experiments, and the LHC data.

DOI: 10.1103/PhysRevD.92.075014 PACS numbers: 98.80.Cq, 12.60.-i

I. INTRODUCTION

The discovery of the Higgs boson at the LHC opens the door for studying the scalar sector of the standard model (SM), and exploring the structure of the scalar sector will be an important task for the LHC in the coming years, which can help us to understand the true mechanism of the electroweak phase transition and the origin of baryon asymmetry of the universe (BAU). The BAU, which has been a long unsolved problem in cosmology and particle physics, is quantified by the baryon-to-photon ratio $\eta = n_B/n_\gamma = 6.05(7) \times 10^{-10}$ [1,2], where n_B and n_γ are the baryon and photon densities, respectively. The observed value of baryon-to-photon ratio can be determined from studies of the power spectrum of the cosmic microwave background radiation or big bang nucleosynthesis. At the end of the inflationary epoch, to generate the BAU (baryogenesis) proposed by Sakarov [3], three conditions must be satisfied: baryon number violation, *C* and *CP*-violation (CPV), and departure from thermal equilibrium or *CPT* violation.

To solve the baryogenesis problem, several mechanisms [i.e., Planck-scale baryogenesis, GUT baryogenesis, leptogenesis, Affleck-Dine bayogenesis, and electroweak baryogenesis (EWB)] have been proposed [4], but after the discovery of the 125 GeV scalar boson [5,6], EWB [7,8] became a popular and testable scenario for explaining the BAU [9]. An important ingredient for the success of EWB is the existence of a strong first order phase transition (SFOPT). However, the 125 GeV Higgs boson is too heavy for efficient SFOPT [9], and there exist three types of extensions of the SM scalar sector to resolve the inefficiency [10]. Another important ingredient is a great enough source of CPV, since the CPV source is too weak in the SM.

In this paper, in the framework of the effective field theory (EFT) (we follow the effective Lagrangian approaches to investigate the EWB in Refs. [11,12]), we introduce a light scalar particle S and an interesting dimension-5 operator $y_t \frac{\eta}{\Lambda} S \bar{Q}_L \tilde{\Phi} t_R + \text{H.c.}$ to provide both the SFOPT and enough CPV for EWB. During the SFOPT ($\langle S \rangle = \sigma$),[1] this dimension-5 operator can provide the CPV source for BAU; then after the SFOPT ($\langle S \rangle = 0$), this operator can naturally avoid the strong constraints from the data of electric dipole moments (EDM) and yield distinctive signals at the LHC, i.e., monojet plus missing transverse energy (MET), mono-Higgs plus MET, and $\bar{t}t$ plus MET. Meanwhile, we will give the constraints on the parameters of the effective Lagrangian from cosmology and particle physics experiments.

In Sec. II, we describe the effective Lagrangian, which can explain the baryogenesis and produce abundant particle phenomenology. In Sec. III, we discuss the realization of the SFOPT in detail, including the constraints from Higgs invisible decay. In Sec. IV, constraints from the observed baryon-to-photon ratio are obtained. In Sec. V, the constraints from the EDM on the new physics (NP) scale are given. In Sec. VI, we investigate the collider constraints on the NP scale at the LHC. Finally, we conclude in Sec. VII.

II. THE EFFECTIVE LAGRANGIAN

Instead of discussing the baryogenesis in a concrete UV-complete theory (such as supersymmetric baryogenesis), which is not easy to make confident predictions about since it has large sets of undetermined additional parameters, we try to explain the BAU and discuss the possible collider signals at the LHC, using EFT. For example, recent studies using the EFT techniques have considered the NP signals at colliders such as monojet, monophoton, and mono-Higgs, recoiling against some MET at colliders. In this paper, we will consider the collider signals of the EWB from the effective Lagrangian:

*csli@pku.edu.cn

[1]In this paper, the angle brackets denote the vacuum expectation value of the field.

$$\mathcal{L} = \mathcal{L}_{\rm SM} + \frac{1}{2}\partial_\mu S \partial^\mu S + \frac{1}{2}\mu^2 S^2 - \frac{1}{4}\lambda S^4 - \frac{1}{2}\kappa S^2(\Phi^\dagger\Phi) + y_t\frac{\eta}{\Lambda} S\bar{Q}_L\tilde{\Phi}t_R + \text{H.c.}, \quad (1)$$

where $\eta = a + ib$ is a complex parameter, $y_t = \sqrt{2}m_t/v$ is the SM top Yukawa coupling, Λ is the NP scale, S is a light singlet scalar particle beyond the SM, Φ is the SM Higgs doublet field, Q_L is the $SU(2)_L$ quark doublet, and t_R is the right-handed top quark. λ and $\lambda_{\rm SM}$ are assumed to be positive here. The similar Lagrangian has been investigated in Refs. [13,14], where the collider phenomenology has not been discussed.

For the effective Lagrangian given in Eq. (1), SFOPT will occur when the vacuum transitions from $(0, \langle S\rangle)$ to $(\langle\Phi\rangle, 0)$, which will be discussed in the following. During the SFOPT, the scalar field S acquires the vacuum expectation value (VEV) as $\langle S\rangle$ and the dimension-5 operator can be rewritten as $\frac{y_t\langle S\rangle}{\sqrt{2}\Lambda}(aH\bar{t}t + ibH\bar{t}\gamma_5 t)$. Thus, the top quark mass gets a spatially varying complex phase along the bubble wall profile [13,14], which provides the source of CPV needed to generate the BAU.

At zero temperature, the VEV of S vanishes and the dimension-5 operator can avoid the electric EDM constraints and induce the interaction term $\frac{m_t}{\Lambda}(aS\bar{t}t + ibS\bar{t}\gamma_5 t)$, which would produce abundant collider signals, such as monojet plus MET, mono-Higgs plus MET, and $\bar{t}t$ plus MET at the LHC.

III. SFOPT

A. Vacuum structure at tree level and zero temperature

Since the phase transition is largely influenced by the vacuum property of the scalar sector at zero temperature, we first study the vacuum structure at tree level and zero temperature. If only the vacuum is considered, we can write the potential as a function of a singlet VEV $\langle S(x)\rangle = \sigma(x)$ and the Higgs field VEV $\langle\Phi(x)\rangle = \frac{1}{\sqrt{2}}(0, H(x))^T$, and we can simplify the potential as

$$V_{\rm tree}(H,\sigma) = -\frac{1}{2}\mu_{\rm SM}^2 H^2 - \frac{1}{2}\mu^2\sigma^2 + \frac{1}{4}\lambda_{\rm SM}H^4 + \frac{1}{4}\lambda\sigma^4 + \frac{1}{4}\kappa H^2\sigma^2. \quad (2)$$

The extremal points can be obtained by the minimization conditions:

$$\left.\frac{\partial V_{\rm tree}}{\partial H}\right|_{(H,\sigma)} = \left.\frac{\partial V_{\rm tree}}{\partial \sigma}\right|_{(H,\sigma)} = 0. \quad (3)$$

Among the nine extremal points, there exist four distinct extremal points as

$$(H,\sigma) = (0,0), \quad (4)$$

$$(H,\sigma) = \left(\frac{\mu_{\rm SM}}{\sqrt{\lambda_{\rm SM}}}, 0\right), \quad (5)$$

$$(H,\sigma) = \left(0, \frac{\mu}{\sqrt{\lambda}}\right), \quad (6)$$

$$(H,\sigma) = \left(\sqrt{\frac{4\lambda\mu_{\rm SM}^2 - 2\kappa\mu^2}{4\lambda\lambda_{\rm SM} - \kappa^2}}, \sqrt{\frac{4\lambda_{\rm SM}\mu^2 - 2\kappa\mu_{\rm SM}^2}{4\lambda\lambda_{\rm SM} - \kappa^2}}\right). \quad (7)$$

The corresponding effective potentials are

$$V(0,0) = 0, \quad (8)$$

$$V\left(\frac{\mu_{\rm SM}}{\sqrt{\lambda_{\rm SM}}}, 0\right) = -\frac{\mu_{\rm SM}^4}{4\lambda_{\rm SM}}, \quad (9)$$

$$V\left(0, \frac{\mu}{\sqrt{\lambda}}\right) = -\frac{\mu^4}{4\lambda}, \quad (10)$$

$$V\left(\sqrt{\frac{4\lambda\mu_{\rm SM}^2 - 2\kappa\mu^2}{4\lambda\lambda_{\rm SM} - \kappa^2}}, \sqrt{\frac{4\lambda_{\rm SM}\mu^2 - 2\kappa\mu_{\rm SM}^2}{4\lambda\lambda_{\rm SM} - \kappa^2}}\right) = \frac{\lambda_{\rm SM}\mu^4 + \lambda\mu_{\rm SM}^4 - \mu^2\mu_{\rm SM}^2\kappa}{\kappa^2 - 4\lambda\lambda_{\rm SM}}. \quad (11)$$

Since λ and $\lambda_{\rm SM}$ are assumed to be positive, then $V\left(\frac{\mu_{\rm SM}}{\sqrt{\lambda_{\rm SM}}}, 0\right) < 0$ and $V(0, \frac{\mu}{\sqrt{\lambda}}) < 0$. For simplicity, we further need $V(0, \frac{\mu}{\sqrt{\lambda}})$ and $V\left(\frac{\mu_{\rm SM}}{\sqrt{\lambda_{\rm SM}}}, 0\right)$ to be the global minima, namely, $V\left(\sqrt{\frac{4\lambda\mu_{\rm SM}^2 - 2\kappa\mu^2}{4\lambda\lambda_{\rm SM} - \kappa^2}}, \sqrt{\frac{4\lambda_{\rm SM}\mu^2 - 2\kappa\mu_{\rm SM}^2}{4\lambda\lambda_{\rm SM} - \kappa^2}}\right) > V\left(\frac{\mu_{\rm SM}}{\sqrt{\lambda_{\rm SM}}}, 0\right)$ and $V\left(\sqrt{\frac{4\lambda\mu_{\rm SM}^2 - 2\kappa\mu^2}{4\lambda\lambda_{\rm SM} - \kappa^2}}, \sqrt{\frac{4\lambda_{\rm SM}\mu^2 - 2\kappa\mu_{\rm SM}^2}{4\lambda\lambda_{\rm SM} - \kappa^2}}\right) > V\left(0, \frac{\mu}{\sqrt{\lambda}}\right)$. These requirements lead to

$$\kappa > 2\sqrt{\lambda\lambda_{\rm SM}}. \quad (12)$$

The degenerate condition of the two minima at tree level is

$$\frac{\mu_{\rm SM}^4}{\lambda_{\rm SM}} = \frac{\mu^4}{\lambda}, \quad (13)$$

which is useful for future discussion of the SFOPT. If $\frac{\mu_{\rm SM}^4}{\lambda_{\rm SM}} > \frac{\mu^4}{\lambda}$, then $V\left(\frac{\mu_{\rm SM}}{\sqrt{\lambda_{\rm SM}}}, 0\right)$ is the only global minimum.

B. Loop and thermal effects

Following the methods in Refs. [15,16], the full finite-temperature effective potential up to one-loop level is composed of three parts,

$$V_{\rm eff}(H,\sigma,T) = V_{\rm tree}(H,\sigma) + V_1^{T=0}(H,\sigma) + \Delta V_1^{T\neq 0}(H,\sigma,T), \quad (14)$$

where $V_{\rm tree}(H,\sigma)$ is the tree-level potential in Eq. (2); $V_1^{T=0}(H,\sigma)$ is the Coleman-Weinberg potential at zero temperature; and $\Delta V_1^{T\neq 0}(H,\sigma,T)$ is the leading thermal correction. Using the high-temperature expansion up to $\mathcal{O}(T^2)$, the effective thermal potential Eq. (14) can be written as

$$V(H,\sigma;T) = D_H(T^2 - T_{0H}^2)H^2 + D_\sigma(T^2 - T_{0\sigma}^2)\sigma^2 + \frac{1}{4}(\lambda_{\rm SM}H^4 + \kappa H^2\sigma^2 + \lambda\sigma^4), \quad (15)$$

with

$$D_H = \frac{1}{32}(8\lambda_{\rm SM} + g'^2 + 3g^2 + 4y_t^2 + 2\kappa),$$
$$D_\sigma = \frac{1}{24}(2\kappa + 5\lambda + 6g_2^2),$$
$$T_{0H}^2 = \frac{\mu_{\rm SM}^2}{2D_H},$$
$$T_{0\sigma}^2 = \frac{\mu^2}{2D_\sigma}.$$

The values of the SM couplings g', g, y_t, and g_2 are chosen according to the results in Ref. [17]. The terms $D_H T^2$ and $D_\sigma T^2$ correspond to the thermal corrections to the mass of H and σ particle, respectively. Here, we omit the thermal contribution of the dimension-5 operator as in Refs. [13,14].

After including the thermal mass effects, the minima of the effective potential become

$$V_{\rm eff}(0,0) = 0, \quad (16)$$

$$V_{\rm eff}\left(\sqrt{\frac{\mu_{\rm SM}^2 - D_H T^2}{\lambda_{\rm SM}}}, 0, T\right) = -\frac{(\mu_{\rm SM}^2 - D_H T^2)^2}{4\lambda_{\rm SM}}, \quad (17)$$

$$V_{\rm eff}\left(0, \sqrt{\frac{\mu^2 - D_\sigma T^2}{\lambda}}, T\right) = -\frac{(\mu^2 - D_\sigma T^2)^2}{4\lambda}, \quad (18)$$

$$V_{\rm eff}\left(\sqrt{\frac{4\lambda\mu_{\rm SM}^2 - 2\kappa\mu^2 - 4\lambda D_H T^2 + 2D_\sigma\kappa T^2}{4\lambda\lambda_{\rm SM} - \kappa^2}}, \sqrt{\frac{4\lambda_{\rm SM}\mu^2 - 2\kappa\mu_{\rm SM}^2 + 2\kappa T^2 D_H - 4D_\sigma T^2\lambda_{\rm SM}}{4\lambda\lambda_{\rm SM} - \kappa^2}}\right) = \frac{T^4\lambda D_H^2 + (\mu^2 - D_\sigma T^2)^2\lambda_{\rm SM} + T^2 D_H(\kappa(\mu^2 - D_\sigma T^2) - 2\lambda\mu_{\rm SM}^2) + \mu_{\rm SM}^2(D_\sigma\kappa T^2 - \kappa\mu^2 + \lambda\mu_{\rm SM}^2)}{\kappa^2 - 4\lambda\lambda_{\rm SM}}. \quad (19)$$

Due to the vacuum structure, the phase transitions take place through two steps: first, S acquires a VEV $\langle S\rangle$, and second, $\langle S\rangle$ vanishes as H acquires a VEV $\langle\Phi\rangle$; i.e., the phase transitions take place as $(0,0) \to (0,\langle S\rangle) \to (\langle\Phi\rangle, 0)$ with the decreasing of the temperature, and SFOPT will occur during the second step from $(0,\langle S\rangle)$ to $(\langle\Phi\rangle, 0)$.

Since the phase transition is dominantly controlled by the tree-level scalar potential, we expect the SFOPT may take place in the vicinity of the degenerate point in Eq. (13). Also, we consider the thermal effects with the small perturbation ($|\delta_{\mu^2}| \ll 1$ and $|\delta_\lambda| \ll 1$) around the degenerate point, which is given by

$$\mu^2 = \mu_{\rm SM}^2\frac{\kappa}{2\lambda_{\rm SM}}(1 + \delta_{\mu^2}), \quad (20)$$

$$\lambda = \left(\frac{\kappa}{2\lambda_{\rm SM}}\right)^2\lambda_{\rm SM}(1 + \delta_\lambda). \quad (21)$$

The critical values can be obtained by substituting Eqs. (20) and (21) into the following expression:

$$V_{\rm eff}(H_c^{(1)}, \sigma_c^{(1)}, T_c) = V_{\rm eff}(H_c^{(2)}, \sigma_c^{(2)}, T_c), \quad (22)$$

and the phase transition critical temperature is given by

$$T_c \approx \frac{m_H\sqrt{\delta_\lambda - 2\delta_{\mu^2}}}{2\sqrt{D_h - D_\sigma}}. \quad (23)$$

From Eqs. (22) and (23), the washout parameter can be obtained as

$$\frac{v(T_c)}{T_c} \approx \frac{2v\sqrt{D_H - D_\sigma}}{m_H\sqrt{\delta_\lambda - 2\delta_{\mu^2}}}. \quad (24)$$

The necessary condition of SFOPT for baryogenesis is

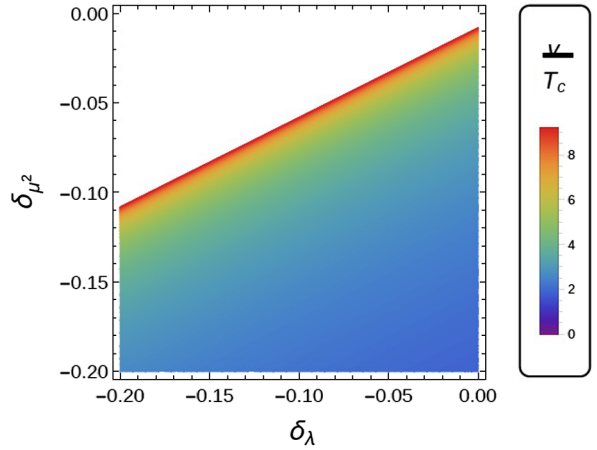

FIG. 1 (color online). The contour plot of the washout parameter v/T_c in the $(\delta_\lambda, \delta_{\mu^2})$ plane.

$$\frac{v(T_c)}{T_c} > 1. \tag{25}$$

From Eq. (24), we see that if $\delta_\lambda - 2\delta_{\mu^2} \ll 1$, $v(T_c)/T_c > 1$ (such as $\delta_\lambda = \delta_{\mu^2} = -0.1$), then the SFOPT can be realized. The dependence of the washout parameter $\frac{v(T_c)}{T_c}$ on δ_λ and δ_{μ^2} is shown in Fig. 1. From Eq. (22), we can get

$$V_{\rm eff}(\sigma, 0, T) - V_{\rm eff}(0, H, T) \approx \frac{\mu_{\rm SM}^4}{4\lambda_{\rm SM}}(\delta_\lambda - 2\delta_{\mu^2}) - \frac{\mu_{\rm SM}^2}{2\lambda_{\rm SM}}(D_H - D_\sigma)T^2. \tag{26}$$

With the decreasing of the temperature, the global minimum of the effective potential changes from $(\sigma, 0)$ to $(0, H)$ and the SFOPT occurs, which can be seen from Eq. (26).

At the critical temperature, there exists a barrier between $(0, \langle S\rangle)$ and $(\langle\Phi\rangle, 0)$, and this leads to the condition $\kappa > 2\sqrt{\lambda\lambda_{\rm SM}}$ at T_c. Substituting Eq. (21) and $|\delta_\lambda| \ll 1$ into this condition, we can get $\kappa > \kappa\sqrt{1+\delta_\lambda}$, which gives $-1 \ll \delta_\lambda < 0$. δ_{μ^2} is also a small negative value to guarantee the positive value of $\delta_\lambda - 2\delta_{\mu^2}$. Note that this constraint of $\kappa > 2\sqrt{\lambda\lambda_{\rm SM}}$ at the critical temperature T_c is ignored in Ref. [10].[2] The mass of the S particle is expressed as

$$m_S^2 = -\frac{\kappa v^2 \delta_{\mu^2}}{2}. \tag{27}$$

Since we consider the phase transition with small perturbation ($|\delta_{\mu^2}| \ll 1$ and $|\delta_\lambda| \ll 1$) around the degenerated point, $|\delta_{\mu^2}|$ and $|\delta_\lambda|$ should be much smaller than 1 as shown in Eqs. (20) and (21). From the viewpoint of the perturbation theory, κ also should be smaller than 1, and thus $|\kappa\delta_{\mu^2}| \ll 1$. From Eq. (27) for the mass of the S particle, the above perturbative requirements for δ_{μ^2} and κ favor a light particle[3] (for example, if $\delta_{\mu^2} = -0.125$ and $\kappa = 0.6$, then $m_S = 47$ GeV), which allows the Higgs invisible decay [10]. The case for the heavy mass has been discussed in Refs. [13,14], and we only study the light scalar case with mass much less than 125 GeV. In this scenario, the portal coupling κ between the singlet S and the Higgs boson can be very small as long as δ_λ and δ_{μ^2} are small negative values, so that it can produce the SFOPT and satisfy the constraints from Higgs invisible decay below.

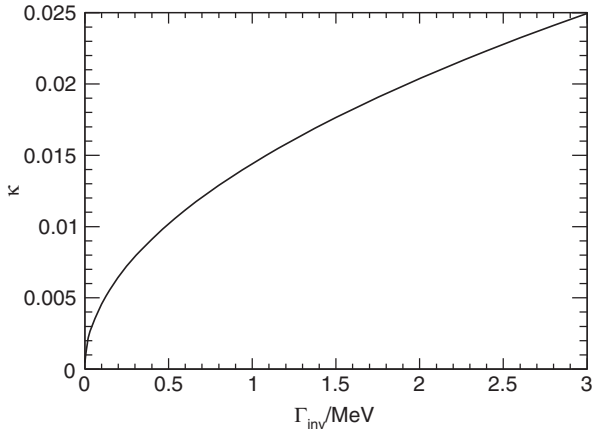

FIG. 2. Upper bounds on the Higgs portal coupling from the Higgs invisible decay width.

C. Higgs invisible decay

After the SFOPT, the VEV of the S field vanishes, and the SM Higgs doublet field Φ can be expanded around the VEV as $\Phi(x) = \frac{1}{\sqrt{2}}(0, \langle\Phi(x)\rangle + H(x))^T$. Substituting this into the Higgs portal term $-\frac{1}{2}\kappa S^2(\Phi^\dagger\Phi)$ in Eq. (1), we obtain the following interaction term,

$$\mathcal{L}_{H\to SS} = -\frac{\kappa\langle\Phi\rangle S^2 H}{4}, \tag{28}$$

which leads to the Higgs invisible decay, and its decay width is

$$\Gamma_{\rm inv}({\rm H}\to{\rm SS}) = \frac{\kappa^2\langle\Phi\rangle^2}{32\pi {\rm m_H}}\sqrt{1-\frac{4{\rm m_S^2}}{\rm m_H^2}} \simeq \frac{\kappa^2\langle\Phi\rangle^2}{32\pi {\rm m_H}}. \tag{29}$$

Figure 2 shows the relation between the Higgs portal coupling κ and $\Gamma_{\rm inv}(H)$. If we take the global fit upper bound of the invisible decay width as [18,19]

$$\Gamma_{\rm inv}({\rm H}) < 1.2\ {\rm MeV}, \tag{30}$$

[2]However, the above constraint is respected in Ref. [13].

[3]The phase transition considered here is similar to the $\overline{\rm E_cSP'}$ case, which favors a light mass [10].

the Higgs portal coupling is constrained as $\kappa < 0.016$ from Eqs. (29) and (30). This constraint indicates that the mass of the S particle should be lighter than 22 GeV from Eq. (27).

IV. CONSTRAINTS FROM THE BARYON-TO-PHOTON RATIO

The BAU depends upon a source of CPV that biases sphaleron interactions near the expanding bubble walls toward baryon production, as opposed to antibaryons [13,14]. Then, inside the bubble walls during the SFOPT, the top quark has a spatially varying complex mass, which is given by [13,14]

$$m_t(z) = \frac{y_t}{\sqrt{2}} H(z)\left(1 + (a + ib)\frac{S(z)}{\Lambda}\right) \equiv |m_t(z)|e^{i\Theta(z)}, \tag{31}$$

where z is taken to be the coordinate transverse to the wall. The CPV phase Θ will provide the source for the BAU, which depends on the sphaleron washout parameter v_c/T_c, the change in VEV σ of the singlet, and the bubble wall thickness L_σ. Using the approximated method in Refs. [13,14], the numerical results can be obtained as shown in Fig. 3, where the baryon-to-photon ratio is defined as

$$\eta_B = \frac{405\Gamma_{\rm sph}}{4\pi^2 v_\sigma g_* T}\int dz \mu_{B_L} f_{\rm sph} e^{-45\Gamma_{\rm sph}|z|/(4v_\sigma)}, \tag{32}$$

and the bubble wall velocity v_σ [20] is chosen as 0.1 and $\Gamma_{\rm sph} \approx 10^{-6}$ T.

From the preliminary numerical estimation in Fig. 3, we see that the observed BAU can be obtained as long as $\sigma/\Lambda < 0.35$. Since the exact calculation of η_B would need improvements of the nonperturbative dynamics, we will discuss how to constrain the NP scale Λ from the EDM data and the LHC data below, which may be more accurate.

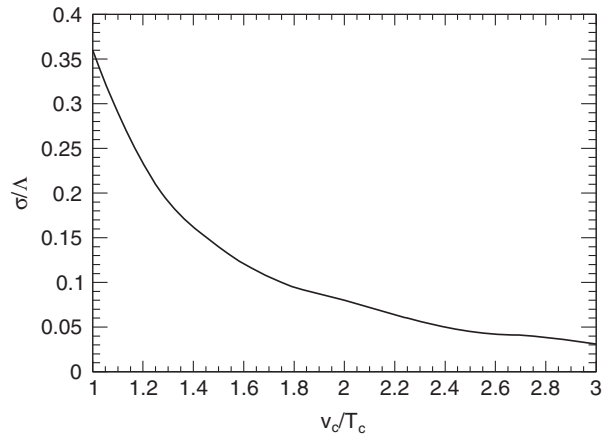

FIG. 3. The approximated numerical relation of the NP scale and the sphaleron washout parameter during the SFOPT to produce the observed baryon-to-photon ratio $\eta = n_B/n_\gamma = 6.05 \times 10^{-10}$ with $L_\sigma v_c = 5$ and $b = 1$.

V. CONSTRAINTS FROM THE NEUTRON EDM

Low-energy CPV probes, such as EDMs, lead to severe constraints on many baryogenesis models. For example, the ACME Collaboration's new result, i.e., $|\frac{d_e}{e}| < 8.7 \times 10^{-29}$ cm at 90% confidence level (C.L.) limit [21], has ruled out a large portion of the parameter space for many baryogenesis models. However, in the case of the considering model in this paper, the strong constraints from the recent electron EDM experiments can be naturally avoided. Due to the fact that S does not acquire a VEV at zero temperature, the mixing of S and the Higgs boson and the CPV interaction of the Higgs-top is prevented; i.e., there are no two-loop Barr-Zee contributions to the electric EDM. Therefore, the dimension-5 operator of the top quark cannot contribute to the electric EDM at the two-loop level.

However, because of the CPV interaction $\frac{m_t}{\Lambda}(aS\bar{t}t + ibS\bar{t}\gamma_5 t)$ between the singlet S and top quark at zero temperature, it can induce the Weinberg operator at the two-loop level, which further gives a contribution to the neutron EDM. The effective Lagrangian is

$$\mathcal{L}_W = \frac{-w}{3} f^{abc} G^a_{\mu\sigma} G^{b,\sigma}_{\nu} \tilde{G}^{c,\mu\nu}, \tag{33}$$

and the corresponding Feynman diagram is shown in Fig. 4. The two-loop matching coefficient w can be expressed as [22–24]

$$w(\mu_W) = \frac{g_s}{4}\frac{\alpha_s}{(4\pi)^3}\sqrt{2}G_F \frac{abv^2}{\Lambda^2} f_3(x_{t/S}). \tag{34}$$

Since the singlet S is very light, $f_3(x_{t/S}) \approx 1$. After performing numerical calculation, the contribution to the neutron EDM is given by

$$\frac{d_n}{e} = (22 \pm 10) \times 2.1 \times 10^{-2} \times \frac{abv^2}{\Lambda^2} \times 10^{-25}\ \text{cm}. \tag{35}$$

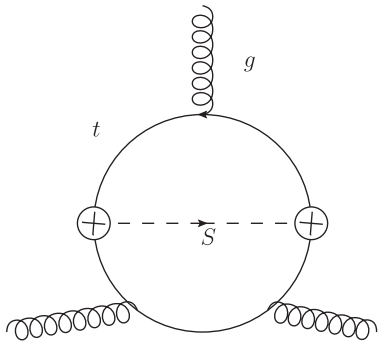

FIG. 4. The contribution to the Weinberg operator at the two-loop level.

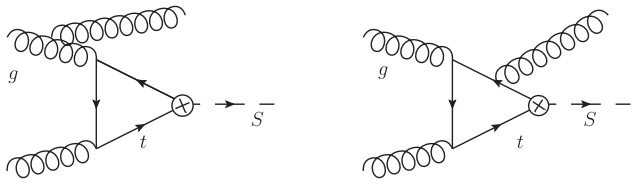

FIG. 5. Sample Feynman diagrams for the monojet plus MET signal.

The 90% C.L. experimental upper bound on the neutron EDM [25] is

$$\left|\frac{d_n}{e}\right| < 2.9 \times 10^{-26}\ \text{cm}, \tag{36}$$

and higher sensitivity is expected from future experiments [26]. After combining the numerical prediction and the experimental bound, we obtain the constraints on the NP scale Λ:

$$\Lambda > [229, 374]\sqrt{ab}\ \text{GeV}. \tag{37}$$

If we choose $a = 1$, $b = 1$, then $\Lambda > [229, 374]$ GeV. From the above discussion, we see that only if it satisfies $a \neq 0$ and $b \neq 0$ simultaneously does a contribution to the neutron EDM exist. If a or b becomes zero, we can also avoid the constraints from the neutron EDM experiments.

VI. CONSTRAINTS FROM THE MONOJET PLUS MET AT THE LHC

At zero temperature, the S field has no VEV, and the Higgs field has a VEV of v. Thus, the dimension-5 operator can induce the operator $\frac{m_t}{\Lambda}(ibS\bar{t}\gamma_5 t + aS\bar{t}\gamma_5 t)$, which can produce the collider signals of mono-Higgs plus MET, top pair plus MET, and monojet plus MET. Considering the current experimental precision for these signals, only the monojet plus MET channel is discussed in this paper to give the precise constraints on the NP scale, since the monojet plus MET channel is the most clean signal among these channels. The other two channels are beyond this paper's scope, and we leave them for a future work. The sample Feynman diagrams for the monojet plus MET signal are shown in Fig. 5, where the S is considered as the MET in collision. The dominant irreducible SM background for monojet plus MET is $Z + j$ production with Z sequentially decaying to neutrino pairs.

In our numerical calculations, we use the recent 19.7 fb^{-1} of 8 TeV CMS results [27], and reconstruct jets using the anti-kt algorithm with radius parameter $R = 0.5$. PYTHIA [28] is used to obtain the parton shower effects. The measurements are performed in seven different MET regions at CMS, and in our case, we find that for the considered interactions the highest sensitivity can be obtained for MET > 500 GeV. The cross section for the monojet plus MET signal at 95% C.L. is given by

$$\sigma(pp \to \text{MET} + \text{jet}) < 6.1\ \text{fb}, \tag{38}$$

and the constraints on the NP scale Λ can be obtained, which are summarized in Table I. We see that the lower limits of the NP scale are about several hundred GeV from current monojet plus MET data. Compared to the constraints from the baryon-to-photon ratio and the EDM, the collider experiments provide more strict constraints on the NP scale.

TABLE I. Sample results of the 95% C.L. lower limits on the NP scale Λ from the CMS analysis [27].

m_S (GeV)	Λ (GeV) for $a = b = 1$ at 8 TeV LHC [27]
6	820
12	500

VII. CONCLUSIONS

The discovery of the 125 GeV scalar particle at the LHC makes the EWB scenario much more realistic and interesting. In this paper, we have investigated the phenomenology of the EWG using EFT by introducing a light scalar particle and a dimension-5 operator. We find that the light scalar field can give SFOPT as long as δ_λ and δ_{μ^2} are small negative values; the dimension-5 operator can provide the CPV source to produce the observed baryon-to-photon ratio during the SFOPT and abundant particle phenomenology. We also discuss the constraints on the NP scale from EDM and LHC data, and show that the extension on the SM with a light scalar particle and a dimension-5 operator can explain the baryogenesis problem in the parameter space allowed by the current EDM and LHC data.

ACKNOWLEDGMENTS

This work was supported by the National Natural Science Foundation of China, under Grants No. 11375013 and No. 11135003.

[1] P. A. R. Ade *et al.* (Planck Collaboration), Astron. Astrophys. **571**, A16 (2014).
[2] K. Olive *et al.* (Particle Data Group), Chin. Phys. C **38**, 090001 (2014).
[3] A. Sakharov, Pis'ma Zh. Eksp. Teor. Fiz. **5**, 32 (1967).
[4] M. Dine and A. Kusenko, Rev. Mod. Phys. **76**, 1 (2003).
[5] G. Aad *et al.* (ATLAS Collaboration), Phys. Lett. B **716**, 1 (2012).
[6] S. Chatrchyan *et al.* (CMS Collaboration), Phys. Lett. B **716**, 30 (2012).
[7] V. Kuzmin, V. Rubakov, and M. Shaposhnikov, Phys. Lett. **B155**, 36 (1985).
[8] M. Trodden, Rev. Mod. Phys. **71**, 1463 (1999).
[9] D. E. Morrissey and M. J. Ramsey-Musolf, New J. Phys. **14**, 125003 (2012).
[10] D. J. Chung, A. J. Long, and L.-T. Wang, Phys. Rev. D **87**, 023509 (2013).
[11] X. Zhang and B. L. Young, Phys. Rev. D **49**, 563 (1994).
[12] X. Zhang, S. K. Lee, K. Whisnant, and B. L. Young, Phys. Rev. D **50**, 7042 (1994).
[13] J. R. Espinosa, B. Gripaios, T. Konstandin, and F. Riva, J. Cosmol. Astropart. Phys. 01 (2012) 012.
[14] J. M. Cline and K. Kainulainen, J. Cosmol. Astropart. Phys. 01 (2013) 012.
[15] M. Quiros, arXiv:hep-ph/9901312.
[16] L. Dolan and R. Jackiw, Phys. Rev. D **9**, 3320 (1974).
[17] D. Buttazzo, G. Degrassi, P. P. Giardino, G. F. Giudice, F. Sala, A. Salvio, and A. Strumia, J. High Energy Phys. 12 (2013) 089.
[18] K. Cheung, J. S. Lee, and P. Y. Tseng, J. High Energy Phys. 05 (2013) 134.
[19] K. Cheung, W. Y. Keung, and T. C. Yuan, Phys. Rev. D **89**, 015007 (2014).
[20] J. Kozaczuk, arXiv:1506.04741.
[21] J. Baron *et al.* (ACME Collaboration), Science **343**, 269 (2014).
[22] D. A. Dicus, Phys. Rev. D **41**, 999 (1990).
[23] E. Braaten, C.-S. Li, and T.-C. Yuan, Phys. Rev. Lett. **64**, 1709 (1990).
[24] D. Chang, W.-Y. Keung, C. S. Li, and T. C. Yuan, Phys. Lett. B **241**, 589 (1990).
[25] C. Baker, D. Doyle, P. Geltenbort, K. Green, M. van der Grinten *et al.*, Phys. Rev. Lett. **97**, 131801 (2006).
[26] T. M. Ito, J. Phys. Conf. Ser. **69**, 012037 (2007).
[27] V. Khachatryan *et al.* (CMS Collaboration), Eur. Phys. J. C **75**, 235 (2015).
[28] T. Sjostrand, S. Mrenna, and P. Z. Skands, Comput. Phys. Commun. **178**, 852 (2008).